Big Data and Neural Networks in Smart Grid - Part 2: The Impact of Piecewise Monotonic Data Approximation Methods on the Performance of Neural Network Identification Methodology for the Distribution Line and Branch Line Length Approximation of Overhead Low-Voltage Broadband over Powerlines Networks

Athanasios G. Lazaropoulos[1,2,*] and Helen C. Leligou[2]

1: School of Electrical and Computer Engineering / National Technical University of Athens / 9 Iroon Polytechniou Street / Zografou, GR 15780
2: Department of Industrial Design and Production Engineering / School of Engineering / University of West Attica / 250 Thivon & P. Ralli / Athens, GR 12244

The impact of measurement differences that follow continuous uniform distributions (CUDs) of different intensities on the performance of the Neural Network Identification Methodology for the distribution line and branch Line Length Approximation (NNIM-LLA) of the overhead low-voltage broadband over powerlines (OV LV BPL) topologies has been assessed in [1]. When the α_{CUD} values of the applied CUD measurement differences remain low and below 5dB, NNIM-LLA may internally and satisfactorily cope with the CUD measurement differences. However, when the α_{CUD} values of CUD measurement differences exceed approximately 5dB, external countermeasure techniques against the measurement differences are required to be applied to the contaminated data prior to their handling by NNIM-LLA. In this companion paper, the impact of piecewise monotonic data approximation methods, such as L1PMA and L2WPMA of the literature, on the performance of NNIM-LLA of OV LV BPL topologies is assessed when CUD measurement differences of various α_{CUD} values are applied. The key findings that are going to be discussed in this companion paper are: (i) The crucial role of the applied numbers of monotonic sections of the L1PMA and L2WPMA for the overall performance improvement of NNIM-LLA approximations as well as the dependence of the applied numbers of monotonic sections on the complexity of the examined OV LV BPL topology classes; and (ii) the performance comparison of the piecewise monotonic data approximation methods of this paper against the one of more elaborated versions of the default operation settings in order to reveal the most suitable countermeasure technique against the CUD measurement differences in OV LV BPL topologies.

1. Introduction

The emerging smart grid that is the upgraded version of the traditional power grid is characterized by its intelligent IP-based communications network of two-way information flows, which may further support a plethora of broadband applications [1]-[10]. Among the communications solutions that can be integrated across the smart grid to support the two-way information flows, Broadband over Power Lines (BPL) networks exploit the available wired power grid infrastructure without the need for investing in extra networking cable across the entire equipment. The integration of the BPL networks with the other communications solutions of the smart grid is feasible through the installation and operation of the BPL wireline / wireless interfaces [4], [8], [11].

Deterministic Hybrid Model (DHM), which describes the BPL signal propagation and transmission across the topologies of the overhead low voltage (OV LV) BPL networks [12]-[20], has acted as the channel model basis while artificial intelligence (AI), machine learning (ML) and neural network (NN) features have been concatenated after it in [1]. Indeed, exploiting the available big data of the Topology Identification Methodology (TIM) BPL topology database for the OV LV BPL topologies of [21], [22] and AI - ML - NN functionalities, the neural network identification methodology for the distribution line and branch line length approximation (NNIM-LLA) has been proposed for the OV LV BPL topologies in [23] while its performance has been assessed in [1] when measurement differences of various intensities may occur. In fact, measurement differences between experimental and theoretical OV LV BPL topology channel attenuation values may be observed due to several practical reasons and "real" life conditions, as shown in [22], [24]. In accordance with [1], [22], [24]-[27], a typical scenario to take into account the measurement differences during the BPL topology channel attenuation analysis is their handling as error distributions, such as the Continuous Uniform Distributions (CUDs) of various amplitudes that are superimposed to the coupling scheme transfer function theoretical numerical results from DHM. In [1], NNIM-LLA has been deployed and benchmarked by exploiting the already knowledge and experience of [3], [23], namely: (i) the list of the indicative OV LV BPL topologies; (ii) default operation settings B of [23]; (iii) default operation settings C of [1]; (iv) the assumption of *a priori* knowledge of the number of branches of the examined indicative OV LV BPL topologies in each case (i.e. not-blind NNIM-LLA approximations); (v) the database representativeness, which is analyzed in [23] for the operation of NNIM-LLA; and (vi) the mechanism proposed in [1] against the unacceptable NNIM-LLA approximations of [23]. In accordance with [3], [23], Root-Mean-Square Deviation (RMSD) has been chosen as the performance metric so that the impact of the measurement differences on the NNIM-LLA approximation performance can be evaluated as well as the countermeasure techniques against them. In [1], it has been revealed that NNIM-LLA presents an inherent mitigation efficiency against CUD measurement differences of low a_{CUD} values (i.e., a_{CUD} values that remain lower than 5dB). In contrast, CUD measurement differences of high a_{CUD} values primarily affect the stability of the NNIM-LLA approximations in terms of their RMSD fluctuations rather than mean RMSD approximations. Also, the adoption of more elaborate default operation settings or representative TIM OV LV BPL topology database sets that are applied separately in each simulation case can significantly improve the stability of the approximations by reducing the RMSD approximation fluctuations but the total duration

time of NNIM-LLA significantly increases. In [1], it has been recognized that the search and the adoption of appropriate countermeasure techniques against measurement differences, such as: (i) smarter countermeasure techniques against measurement differences prior to the application of the NNIM-LLA module; and (ii) tailored-made and representative segments of the TIM OV LV BPL database that holds per case groups and not per examined case. Among the available countermeasure techniques against measurement differences prior to the application of the NNIM-LLA module, the piecewise monotonic data approximation methods are assessed in this companion paper so as to improve the performance of NNIM-LLA approximations in terms of the RMSD fluctuations, mean RMSD and the total duration time.

From the literature, the application of piecewise monotonic data approximation methods, such as L1PMA and L2WPMA which have theoretically been presented and experimentally verified in [28]-[33], may successfully cope with the measurement differences. In accordance with [25], L1PMA and L2WPMA are formally categorized in the piecewise monotonic data approximations with predefined monotonic sections. L1PMA and L2WPMA have been proposed in [31]-[35] while their performance regarding the mitigation of measurement differences in transmission and distribution BPL networks has been assessed in [22], [24], [25], [27], [28], [36], [37] as output module after the DHM one. Already been identified in [22], [24], [25], [27], [36], the performance of L1PMA and L2WPMA mainly depends on the predefined number of monotonic sections while their best approximation performance against measurement differences is achieved when a specific number of monotonic sections can be identified and applied per measurement difference case. Acknowledging that the right selection of the number of monotonic sections plays the key role during the application of L1PMA and L2WPMA, the findings of [25], [27] concerning the adaptive number of monotonic sections during the operation of L1PMA and L2WPMA are going to be checked in this companion paper. Hence, the piecewise monotonic data approximation module (PMDAM), which consists of either L1PMA or L2WPMA, is concatenated after the DHM module but before the NNIM-LLA one in this companion paper. NNIM-LLA performance against CUD measurement differences is going to be assessed in terms of RMSD fluctuations, mean RMSD and total duration time when the PMDAM is added. Useful conclusions are expected through the comparison of RMSD fluctuations, mean RMSD and total duration time achieved by L1PMA and L2WPMA with the respective ones of [1], say, achieved by the application of default operation settings B (default operation settings basis) and default operation settings C.

The rest of this companion paper is organized as follows: Section 2 briefly presents L1PMA and L2WPMA as well as their integration in the NNIM-LLA operation through the PMDAM and DHM. In Section 3, the numerical results regarding the impact of measurement differences on the approximation performance of NNIM-LLA are given. The mitigation role of the three scenarios against the CUD measurement differences is assessed in terms of the RMSD fluctuations, mean RMSD and NNIM-LLA total duration time. Section 4 concludes this companion paper.

2. PMDAM

In this Section, the adoption of L1PMA and L2WPMA is detailed under the aegis of the PMDAM. As the PMDAM is considered as a countermeasure technique module

against the CUD measurement differences of [1], its location across the NNIM-LLA operation flowchart stands right after the theoretical coupling scheme channel transfer function results of DHM that are contaminated by CUD measurement differences (say, measured coupling scheme channel transfer function results) for given examined OV LV BPL topology. Depending on the applied piecewise monotonic data approximation method of PMDAM, PMDAM input is the aforementioned measured coupling scheme channel transfer function results while PMDAM output is the respective approximated coupling scheme channel transfer function results, which are ideally equal to the theoretical coupling scheme channel transfer function results of the examined OV LV BPL topology [22], [24], [25], [27], [28], [36]. Practically, instead of the measured coupling scheme channel transfer function results of the examined OV LV BPL topology, NNIM-LLA receives as input the respective approximated coupling scheme channel transfer function results without affecting the applied representative sets of the TIM OV LV BPL topology database and the operation of the MATLAB NN program of [38], [39], which programmatically supports the fully connected NN architecture of Figure 2 of [3] as well as the involved training, validation and testing phases. The efficient performance of piecewise monotonic data approximations entails lower RMSD fluctuations that ideally tend to zero. As the total duration time is concerned, the representative sets of the TIM OV LV BPL topology database are prepared per each examined case and the default operation settings B are assumed as the default operation settings basis, it is expected that the total duration time after the application of piecewise monotonic data approximation methods as countermeasure technique against the CUD measurement differences of [1] remains closer to the one after the application of default operation settings B rather than the one of default operation settings C. In the following two subsections, a brief presentation of L1PMA and L2WPMA is given.

2.1 L1PMA

L1PMA is the first one of the two piecewise monotonic data approximations supported by PMDAM in this companion paper. L1PMA is going to exploit the piecewise monotonicity property of the theoretical coupling scheme channel transfer function results of DHM by decomposing the previous results into separate monotonous sections between their adjacent turning points (primary extrema) for given OV LV BPL topology [28], [32], [33], [36]. Aiming at minimizing the moduli sum of the CUD measurement differences, L1PMA is going to mitigate the uncorrelated measurement differences by neglecting the existence of few large ones [28]. A detailed analysis concerning the extensive application of L1PMA to transmission and distribution BPL networks is given in [22], [24], [25], [27], [28], [36], [40]. Already been reported for PMDAM, L1PMA receives as inputs the measured coupling scheme channel transfer function results of the examined OV LV BPL topology, the measurement frequencies and the number of monotonic sections (i.e., either user- or computer-defined) and gives as output the best fit of the measured OV MV BPL coupling transfer function results; say, the respective L1PMA approximated coupling scheme channel transfer function results. Note that the measurement frequencies and the findings concerning the applied number of monotonic sections, which have been presented in [40] and treat with the application of L1PMA to OV LV BPL topologies, are going to be exploited in this companion paper.

2.2 L2WPMA

L2PMA is the second one of the two piecewise monotonic data approximations supported by PMDAM in this companion paper. In accordance with [37] and similarly to L1PMA of Sec.2.1, L2WPMA is going to decompose the examined input data of the measured coupling scheme channel transfer function of the examined OV LV BPL topology into separate monotonous sections between its primary extrema [25], [35], [36]. Apart from the measured data, L2WPMA software receives as input the measurement frequencies and the number of monotonic sections, similarly to L1PMA, and gives as output a spline representation of the measured data. Conversely to L1PMA, L2WPMA focuses on the first divided of the input measured data by demanding the minimization of the weighted sum of the square of the measurement differences via the constraint of specific number of sign changes [25], [27], [35], [36]. The number of sign changes is equal to the number of monotonic sections minus one where the number of monotonic sections is either user- or computer-defined in a similar way to L1PMA.

3. Numerical Results and Discussion

In this Section, the mitigation role of the piecewise monotonic data approximations, say, L1PMA and L2WPMA, against the CUD measurement differences of different intensities is investigated. In fact, the default operation settings that are adopted in this companion and remain almost identical to the ones of the original paper of [1] are initially detailed. The small differences in default operation settings B (basis) and default operation settings C are due to the restrictions in software use of L1PMA and L2WPMA. Then, the L1PMA and L2WPMA of different number of monotonic sections, in compliance with the findings of [25], [27], are deployed against the CUD measurement differences of different intensities. The results of the application of the piecewise monotonic data approximations of PMDAM of this companion paper are presented and discussed in terms of the RMSD approximation fluctuations and the total duration time of NNIM-LLA when are compared against the results produced by the simple application of the default operation settings B (basis) and default operation settings C.

3.1 Default Operation Settings

According to [1], the default operation settings define the values of the maximum number of branches N_{max}, the length spacing L_s for both the branch distance and the branch length, the maximum branch length $L_{b,max}$ and the operation frequency range that are anyway essential factors for the five fields of TIM OV LV BPL topology database that are used during the operation of NNIM-LLA. As the maximum number of branches, the length spacing and the maximum branch length are concerned, these remain the same when the default operation settings B and C are applied in this companion paper. However, in order to comply with the requirement of the Fortran software that supports the piecewise monotonic data approximations of this companion paper [33], [35], small changes are required in the frequency range and the flat-fading subchannel frequency spacing; say, the BPL frequency range and flat-fading subchannel frequency spacing are assumed equal to 1-30MHz and 1MHz, respectively, in [25], [36]. To prevent the misunderstanding of the results of the following subsections with the results of the original paper, default operation settings B' and C' are denoted hereafter for the default operation settings B and C of [1], respectively.

Except for the previous default operation settings, the following assumptions of [1] are also taken into account in this companion paper, namely: (i) The number of branches of the examined indicative OV LV BPL topologies (say, suburban and rural cases of Table 1 of [1]) is assumed to be known; (ii) the database representativeness, which is analyzed in [23] for the operation of NNIM-LLA, is assumed during the application of the default operation settings B' and C'; (iii) the exclusion of the symmetrical OV LV BPL topologies from the OV LV BPL topology database so as not to disrupt the approximations due to the symmetry of BPL topologies described in [41], [42]; (iv) the inclusion of the examined suburban and rural cases into the TIM OV LV BPL topology database; and (v) the mechanism described in [1] for preventing the unacceptable NNIM-LLA approximations of [23] (i.e., at least one of the approximated distribution and branch line lengths is below zero given the fixed length of 1000m between the transmitting and receiving ends for all the applied OV LV BPL topologies).

Finally, it should be noted that the default participation percentages of the three phases of NNIM-based methodologies of [3], [23], [38], [39] are assumed in this paper; say, training, validation and testing phases during the operation of NNIM-LLA are assumed to be equal to 70%, 15% and 15%, respectively.

3.1.1 Default Operation Settings B'

As the impact of CUD measurement differences on the performance of NNIM-LLA is investigated, similarly to Table 6 of [1], in Table 1, given the amplitudes of coupling scheme channel transfer functions contaminated with measurements in dB for the suburban case, NNIM-LLA gives as output its respective approximations of the distribution and branch line lengths when various a_{CUD} values of CUD measurements are assumed. Conversely to Table 6 of [1], note that one $1 \times Q = 1 \times (30 - 1) = 1 \times 29$ measurement difference line vector for each a_{CUD} value that ranges from 0dB to 20dB is superimposed to the amplitudes of the coupling scheme channel transfer functions of the suburban case for the respective NNIM-LLA approximation cases. Also, the best RMSD value between the approximated original and symmetrical OV LV topologies and the respective OV LV BPL topology are presented per a_{CUD} value in Table 1. Table 2 is similar to Table 1 but for the rural case. Note that the same 21×29 measurement difference vector with Table 1 is here superimposed to the amplitudes of the coupling scheme channel transfer functions of the rural case for all the examined NNIM-LLA approximation cases. In Tables 1 and 2, the default operation settings B' are applied when one hidden layer is assumed during the NNIM-LLA simulations, as analyzed in [1].

From Tables 1 and 2, the fluctuating RMSD value trend that is not directly correlated with the examined a_{CUD} values, which has first been observed in [1], is also seen in this companion paper when different a_{CUD} values for the CUD measurements are applied in the suburban and rural cases. Indeed, with reference to Table 1, the maximum RMSD difference between the best values for the suburban case is equal to 137.95m when one hidden layer is assumed and a_{CUD} values range from 1dB to 20dB. As the rural case is concerned in Table 2, maximum RMSD difference between the best values is equal to 127.26m when one hidden layer is assumed and a_{CUD} values range from 1dB to 20dB. Note that the respective maximum RMSD difference of Tables 6 and 7 in [1] was equal to 157.10m.and 187.72m for the suburban and rural cases, respectively, when a_{CUD} values range from 0dB to 20dB. Similarly to [1], the intrinsic mitigation characteristic of

Table 1

Distribution and Branch Line Length Approximations of NNIM-LLA for the Suburban Case and Default Operation Settings B' for Different a_{CUD} Values of CUD Measurements (the symmetrical approximations are reported in blue font color and the suburban case is included in the TIM OV LV BPL topology database)

Indicative OV LV BPL Topologies of Table 1 of [1]		Suburban Case	RMSD	Notes
Distribution Line Length L $=[L_1 \quad L_2 \quad L_3 \quad 0]$ **Branch Line Length L$_b$** $=[L_{b1} \quad L_{b2} \quad 0]$		[500m 400m 100m 0m] [50m 10m 0m]	-	-
NNIM-LLA **Approximated Distribution Line Length** $\mathbf{L_{NNIM-LLA}} =$ $[L_{1,NNIM-LLA} \quad L_{2,NNIM-LLA} \quad L_{3,NNIM-LLA} \quad 0]$ **Approximated Branch Line Length** $\mathbf{L_{b,NNIM-LLA}} =$ $[L_{b1,NNIM-LLA} \quad L_{b2,NNIM-LLA} \quad 0]$	a_{CUD} **of CUD Measurements (dB)**			Default Operation Settings B' + 1 hidden layer
	0	[36]4.46m 72.13m 213.41m 0m] [148.890m 147.42m 0m]	166.91m	
	1	[213.23m 731.29m 55.49m 0m] [171.73m 135.05m 0m]	179.06m	
	2	[405.62m 491.25m 103.13m 0m] [157.74m 147.86m 0m]	82.68m	
	3	[224.99m 717.42m 57.59m 0m] [169.55m 150.48m 0m]	174.11m	
	4	[213.40m 736.27m 50.33m 0m] [157.45m 120.47m 0m]	177.86m	
	5	[721.98m 65.59m 212.43m 0m] [147.66m 137.09m 0m]	168.79m	
	6	[706.71m 80.54m 212.75m 0m] [164.17m 172.26m 0m]	167.70m	
	7	[147.59m 830.84m 21.53m 0m] [143.29m 136.76m 0m]	220.63m	
	8	[744.82m 33.54m 221.64m 0m] [162.64m 151.99m 0m]	185.88m	
	9	[700.03m 103.25m 196.72m 0m] [156.13m 147.66m 0m]	154.75m	
	10	[701.72m 97.38m 200.90m 0m] [135.33m 141.61m 0m]	154.48m	
	11	[666.52m 134.99m 198.50m 0m] [152.01m 141.36m 0m]	139.04m	
	12	[618.06m 201.75m 180.19m 0m] [161.76m 153.20m 0m]	115.06m	
	13	[231.12m 708.62m 60.26m 0m] [158.41m 129.19m 0m]	166.94m	
	14	[708.95m 83.73m 0m] [151.95m 153.28m 0m]	163.06m	
	15	[267.66m 159.70m 174.12m 0m] [301.11m 165.48m 0m]	170.90m	
	16	[690.06m 118.57m 191.37m 0m] [132.96m 149.55m 0m]	146.40m	
	17	[162.82m 818.26m 18.85m 0m] [127.85m 128.08m 0m]	212.21m	
	18	[677.14m 132.21m 190.65m 0m] [145.84m 144.05m 0m]	140.64m	
	19	[36]9.34m 64.14m 216.52m 0m] [158.07m 139.60m 0m]	170.28m	

	20	[214.14m 739.62m 46.24m 0m] [166.20m 141.49m 0m]	181.56m	

Table 2
Distribution and Branch Line Length Approximations of NNIM-LLA for the Rural Case and Default Operation Settings B' for Different a_{CUD} Values of CUD Measurements (the symmetrical approximations are reported in blue font color and the rural case is included in the TIM OV LV BPL topology database)

Indicative OV LV BPL Topologies of Table 1 of [1]		Rural Case	RMSD	Notes
Distribution Line Length L $=[L_1 \quad L_2 \quad 0 \quad 0]$ **Branch Line Length L$_b$** $=[L_{b1} \quad 0 \quad 0]$		[600m 400m 0m 0m] [300m 0m 0m]	-	-
NNIM-LLA **Approximated Distribution Line Length** $\mathbf{L_{NNIM-LLA}} = [L_{1,NNIM-LLA} \quad L_{2,NNIM-LLA} \quad 0 \quad 0]$ **Approximated Branch Line Length** $\mathbf{L_{b,NNIM-LLA}} = [L_{b1,NNIM-LLA} \quad 0 \quad 0]$	a_{CUD} **of CUD Measurements (dB)**			Default Operation Settings B' + 1 hidden layer
	0	[36]1.15m 288.85m 0m 0m] [167.16m 0m 0m]	77.78m	
	1	[700.35m 299.69m 0m 0m] [18.16m 0m 0m]	119.26m	
	2	[628.82m 255.02m 0m 0m] [320.21m 0m 0m]	56.39m	
	3	[732.97m 267.31m 0m 0m] [157.15m 0m 0m]	89.20m	
	4	[582.56m 417.44m 0m 0m] [29.11m 0m 0m]	102.81m	
	5	[678.36m 320.46m 0m 0m] [135.46m 0m 0m]	75.16m	
	6	[824.04m 382.54m 0m 0m] [181.65m 0m 0m]	96.00m	
	7	[548.71m 318.94m 0m 0m] [62.44m 0m 0m]	96.83m	
	8	[635.77m 281.28m 0m 0m] [80.30m 0m 0m]	95.35m	
	9	[780.97m 218.95m 0m 0m] [356.41m 0m 0m]	99.08m	
	10	[630.51m 346.01m 0m 0m] [483.88m 0m 0m]	73.35m	
	11	[888.77m 119.76m 0m 0m] [193.03m 0m 0m]	157.37m	
	12	[700.03m 300.01m 0m 0m] [208.74m 0m 0m]	63.62m	
	13	[748.51m 251.49m 0m 0m] [106.72m 0m 0m]	107.88m	
	14	[700.61m 275.78m 0m 0m] [143.78m 0m 0m]	84.48m	
	15	[741.43m 258.36m 0m 0m] [158.01m 0m 0m]	92.76m	
	16	[904.25m 95.90m 0m 0m] [74.08m 0m 0m]	183.65m	
	17	[720.42m 512.40m 0m 0m] [309.69m 0m 0m]	62.37m	

	18	[800.02m 223.20m 0m 0m] [158.85m 0m 0m]	114.14m	
	19	[524.16m 507.58m 0m 0m] [614.82m 0m 0m]	128.97m	
	20	[737.50m 262.50m 0m 0m] [150.00m 0m 0m]	92.82m	

NNIM-LLA against the measurement differences is more affected by the TIM OV LV BPL topology database representativeness in terms of the topology characteristics rather than the accuracy of the assumed frequency range. The latter observation is verified by the comparable maximum RMSD differences between the best values when the two different frequency range of 3-88MHz of [1] and 1-30MHz of this companion paper are assumed for the suburban and rural cases of Tables 1 and 2, respectively. As the mean RMSD values of Tables 1 and 2 are concerned for the a_{CUD} values that range from 1dB to 20dB, these are equal to 163.60m and 99.57m for the suburban and rural case, respectively. Note that the total duration time for preparing both Tables 1 and 2 is equal to 1,342s for the default operation settings B' of the frequency range of 1-30MHz while the respective total duration time for the default operation settings B of the frequency range of 3-88MHz was equal to 3,505s as reported in [1]. The previous total duration time difference is mainly due to the operation of the MATLAB NN program of [38], [39] that programmatically supports the fully connected NN architecture of NNIM-LLA as well as the involved training, validation and testing phases.

3.1.2 Default Operation Settings C'

In accordance with [1], the higher accuracy degree of the TIM OV LV BPL topology database, which is affected by the adoption of the default operation settings C, has significantly improved the RMSD fluctuations by reducing the maximum RMSD differences of the NNIM-LLA approximations when the a_{CUD} values range from 1dB to 20dB. Also, the default operation settings C has slightly improved mean RMSD values for given examined indicative OV LV BPL topology. But the adoption of the default operation settings C entailed higher duration times of NNIM-LLA in [1] when the preparation of the TIM OV LV BPL topology database is made from the beginning in each examined case.

Similarly to Table 1, NNIM-LLA gives approximations of the distribution and branch line lengths in Table 4 when the default operation settings C' are adopted and the same a_{CUD} values of CUD measurements of Table 1 are assumed. The same 21×29 measurement difference vector with Tables 1 and 2 is here superimposed to the amplitudes of the coupling scheme channel transfer functions of the suburban case for all the 21 NNIM-LLA approximation cases. Similarly to Table 1, the best RMSD value between the approximated original and symmetrical OV LV topologies and the respective OV LV BPL topology are presented per a_{CUD} value in Table 3. Table 4 is similar to Table 3 but for the rural case.

Table 3
Distribution and Branch Line Length Approximations of NNIM-LLA for the Suburban Case and Default Operation Settings C' for Different a_{CUD} Values of CUD Measurements (the symmetrical approximations are reported in blue font color and the suburban case is included in the TIM OV LV BPL topology database)

Indicative OV LV BPL Topologies of Table 1 of [1]		Suburban Case	RMSD	Notes
Distribution Line Length L =$[L_1 \quad L_2 \quad L_3 \quad 0]$ **Branch Line Length L$_b$** =$[L_{b1} \quad L_{b2} \quad 0]$		[500m 400m 100m 0m] [50m 10m 0m]	-	-
NNIM-LLA **Approximated Distribution Line Length** $\mathbf{L}_{NNIM-LLA} =$ $[L_{1,NNIM-LLA} \quad L_{2,NNIM-LLA} \quad L_{3,NNIM-LLA} \quad 0]$ **Approximated Branch Line Length** $\mathbf{L}_{b,NNIM-LLA} =$ $[L_{b1,NNIM-LLA} \quad L_{b2,NNIM-LLA} \quad 0]$	a_{CUD} **of CUD Measurements (dB)**			Default Operation Settings C' + 1 hidden layer
	0	[627.845m 189.99m 182.16m 0m] [147.73m 140.07m 0m]	115.68m	
	1	[573.93m 265.68m 160.39m 0m] [158.32m 147.37m 0m]	90.83m	
	2	[630.92m 189.36m 179.72m 0m] [148.02m 139.35m 0m]	116.01m	
	3	[567.68m 270.96m 161.36m 0m] [156.08m 149.47m 0m]	89.20m	
	4	[234.82m 724.03m 41.16m 0m] [125.29m 111.39m 0m]	166.79m	
	5	[303.84m 620.03m 76.12m 0m] [135.79m 127.45m 0m]	124.57m	
	6	[567.25m 272.78m 159.97m 0m] [157.14m 149.64m 0m]	88.87m	
	7	[571.01m 266.27m 162.71m 0m] [156.06m 146.84m 0m]	90.10m	
	8	[223.63m 731.26m 45.11m 0m] [168.40m 159.68m 0m]	179.50m	
	9	[575.78m 259.46m 164.76m 0m] [148.27m 138.48m 0m]	89.33m	
	10	[239.14m 711.14m 49.72m 0m] [128.35m 122.70m 0m]	163.11m	
	11	[569.29m 266.80m 163.91m 0m] [156.69m 148.66m 0m]	90.43m	
	12	[567.31m 272.21m 160.48m 0m] [157.04m 149.03m 0m]	88.89m	
	13	[569.82m 269.94m 160.24m 0m] [159.05m 150.65m 0m]	90.31m	
	14	[572.51m 263.54m 163.95m 0m] [153.36m 144.36m 0m]	90.00m	
	15	[272.11m 665.07m 62.82m 0m] [126.67m 117.14m 0m]	141.89m	
	16	[629.36m 189.32m 181.31m 0m] [146.02m 142.22m 0m]	116.15m	
	17	[569.76m 269.09m 161.15m 0m] [157.22m 149.08m 0m]	89.91m	
	18	[566.49m 273.58m 159.93m 0m] [156.31m 149.37m 0m]	88.42m	
	19	[632.95m 188.14m 178.91m 0m] [147.73m 142.46m 0m]	117.03m	

| | 20 | [210.58m 743.53m 45.89m 0m] [145.86m 130.88m 0m] | 180.68m | |

Table 4

Distribution and Branch Line Length Approximations of NNIM-LLA for the Rural Case and Default Operation Settings C' for Different a_{CUD} Values of CUD Measurements (the symmetrical approximations are reported in blue font color and the rural case is included in the TIM OV LV BPL topology database)

Indicative OV LV BPL Topologies of Table 1 of [1]		**Rural Case**	**RMSD**	**Notes**
Distribution Line Length L $=[L_1 \quad L_2 \quad 0 \quad 0]$ **Branch Line Length L$_b$** $=[L_{b1} \quad 0 \quad 0]$		[600m 400m 0m 0m] [300m 0m 0m]	-	-
NNIM-LLA **Approximated Distribution Line Length** $L_{NNIM-LLA} = [L_{1,NNIM-LLA} \quad L_{2,NNIM-LLA} \quad 0 \quad 0]$ **Approximated Branch Line Length** $L_{b,NNIM-LLA} = [L_{b1,NNIM-LLA} \quad 0 \quad 0]$	a_{CUD} **of CUD Measurements (dB)**			Default Operation Settings C' + 1 hidden layer
	0	[726.55m 251.36m 0m 0m] [108.88m 0m 0m]	103.26m	
	1	[748.48m 251.54m 0m 0m] [346.36m 0m 0m]	81.27m	
	2	[793.83m 206.16m 0m 0m] [202.98m 0m 0m]	109.91m	
	3	[767.26m 246.89m 0m 0m] [154.48m 0m 0m]	101.84m	
	4	[735.21m 277.30m 0m 0m] [116.69m 0m 0m]	97.79m	
	5	[373.28m 605.60m 0m 0m] [16.22m 0m 0m]	157.75m	
	6	[730.68m 269.01m 0m 0m] [180.13m 0m 0m]	83.33m	
	7	[772.27m 227.73m 0m 0m] [204.96m 0m 0m]	98.84m	
	8	[627.09m 421.38m 0m 0m] [155.14m 0m 0m]	56.29m	
	9	[694.73m 302.17m 0m 0m] [175.22m 0m 0m]	69.81m	
	10	[706.80m 296.86m 0m 0m] [157.79m 0m 0m]	77.705m	
	11	[733.03m 266.97m 0m 0m] [41.41m 0m 0m]	120.87m	
	12	[795.07m 204.92m 0m 0m] [339.34m 0m 0m]	105.33m	
	13	[788.62m 206.09m 0m 0m] [162.14m 0m 0m]	114.76m	
	14	[605.60m 373.28m 0m 0m] [16.22m 0m 0m]	107.75m	
	15	[654.23m 374.86m 0m 0m] [149.29m 0m 0m]	61.28m	
	16	[764.86m 235.14m 0m 0m] [125.68m 0m 0m]	110.03m	
	17	[674.54m 276.29m 0m 0m] [53.44m 0m 0m]	108.00m	

	18	[27]2.63m 317.37m 0m 0m] [441.75m 0m 0m]	69.44m	
	19	[877.89m 276.24m 0m 0m] [191.15m 0m 0m]	122.12m	
	20	[737.27m 258.02m 0m 0m] [152.23m 0m 0m]	93.22m	

According to [1], the adoption of default operation settings that create more elaborate versions of the TIM OV LV BPL topology database, such as the default operation settings C' of this Section against the default operation settings B' of Sec.3.1.1, improves the NNIM-LLA approximation performance but the preparation of the TIM OV LV BPL topology database, which is assumed in [1] and this companion paper, entails prohibitive total duration times when even more elaborate default operation settings need to be assumed. With reference to Table 3, the maximum RMSD difference between the best values for the suburban case is equal to 92.26m when the default operation settings C' are applied, one hidden layer is assumed and a_{CUD} values range from 1dB to 20dB while the respective maximum RMSD difference between the best values is equal to 137.95m when the default operation settings B' has been applied in Table 1. Similarly to the suburban case, as the rural case is concerned in Table 4, maximum RMSD difference between the best values is equal to 93.71m when the default operation settings C' are applied, one hidden layer is assumed and a_{CUD} values range from 1dB to 20dB while the respective maximum RMSD difference between the best values is equal to 127.26m when the default operation settings B' has been applied in Table 2. Apart from the maximum RMSD difference between the best values, the default operation settings C' also improve the mean RMSD metrics; say, the mean RMSDs between the best values for the suburban case of Table 3 and rural case of Table 4 are equal to 114.60m and 96.98m, respectively, when the default operation settings C' are applied, one hidden layer is assumed and a_{CUD} values range from 1dB to 20dB while the respective mean RMSDs of Tables 1 and 2 are equal to 163.60m and 99.57m when the default operation settings B' has been applied. Therefore, it is evident that the adoption of more elaborate default operation settings is a fine countermeasure technique against the measurement differences of various a_{CUD} values that anyway enhances the intrinsic mitigation characteristics of NNIM-LLA. However, the slight positive impact of the elaborate default operation settings on the RMSD metrics is explained by the representativeness of the OV LV BPL topologies in the TIM OV LV BPL topology databases that remains unaffected either in the suburban case or in rural one [1], [3], [23]. Note that the total duration time for preparing both Tables 3 and 4 is equal to 10,048s for the default operation settings C' of the frequency range of 1-30MHz while the respective total duration time for the default operation settings C of the frequency range of 3-88MHz was equal to 29,364s as reported in [1]. Again, similarly to the default operation settings C and B of [1], the total duration time for preparing both Tables 3 and 4 is increased by approximately three times in comparison with the total duration time for preparing both Tables 1 and 2 and this is clearly due to the operation of the NNIM-LLA as well as the involved training, validation and testing phases.

3.2 L1PMA and L2WPMA of PMDAM

Already been identified in [22], [24], [25], [27], [36], the mitigation performance of L1PMA and L2WPMA against measurement differences mainly depends on the predefined number of monotonic sections. In accordance with [25], [27], different numbers of monotonic sections can be applied depending on the examined BPL topology class and the applied a_{CUD} value when deterministic and statistic systems are examined. Here, the mitigation performance of L1PMA and L2WPMA against measurement differences is assessed when the measurement differences of various a_{CUD} values are applied and default operation settings B' are assumed but PMDAM, which consists of piecewise monotonic data approximations, precedes the NNIM-LLA module. Except for the mitigation performance, the total duration time of the integration of the default operation settings B', PMDAM and NNIM-LLA is compared against the total duration time of the operation of the default operation settings C' and NNIM-LLA.

As the effect of the number of monotonic sections is investigated in L1PMA, in Table 5, the maximum RMSD difference between the best values and mean RMSD for the suburban case is reported per monotonic section, which ranges from 1 to 20, when L1PMA is applied and a_{CUD} values of measurement differences range from 1dB to 20dB. In Table 6, similar approximation performance metrics are given but for the rural case. Note that the same measurement difference vector with Tables 1 and 2 is here superimposed to the amplitudes of the coupling scheme channel transfer functions of the suburban and rural cases for all the NNIM-LLA approximation cases. Apart from the aforementioned approximation performance metrics, for comparison reason, the maximum RMSD difference between the best values and mean RMSD are reported when the default operation settings B' and C' are applied in each examined case.

In Tables 5 and 6, the maximum RMSD difference between the best values and the mean RMSD that are lower than the respective values of the default operation settings B' per case are shown in green color while the cases with the lowest maximum RMSD difference between the best values are highlighted in yellow color. As the suburban case of Table 5 is concerned, L1PMA mainly helps towards the improvement of mean RMSD rather than of the maximum RMSD difference between the best values while the opposite holds in the rural case of Table 6. In accordance with [25], [27], the careful selection of the number of monotonic sections is critical for achieving the measurement difference mitigation and this number primarily depends on the examined BPL topology complexity; say, for the suburban and rural cases, 20 and 6 monotonic sections have been respectively applied in [25], [27]. Due to the higher complexity of the suburban case concerning the number of the branches, higher number of monotonic sections is here required in contrast with the rural case. Indeed, with reference to Tables 5 and 6, 10 and 6 monotonic sections achieve the lowest maximum RMSD difference between the best values for the suburban and rural case, respectively; the previous values for the monotonic sections agree with the concept presented in [25], [27].

Table 5

Distribution and Branch Line Length Approximations of NNIM-LLA for the Suburban Case and Default Operation Settings B' for Different L1PMA Numbers of Monotonic Sections when a_{CUD} Values of CUD Measurements range from 1dB to 20dB

L1PMA Number of Monotonic Sections	Maximum RMSD Difference between the Best Values (m) (Default Operation Settings B': 137.95m) (Default Operation Settings C': 92.26m)	Mean RMSD (m) (Default Operation Settings B': 163.60m) (Default Operation Settings C': 114.60m)
1	209.74	166.42
2	213.38	163.84
3	133.41	164.72
4	186.07	180.41
5	186.82	153.33
6	146.45	173.01
7	335.68	156.29
8	202.05	147.61
9	217.04	159.22
10	132.31	158.89
11	193.60	163.39
12	143.01	165.39
13	174.36	158.81
14	188.72	150.15
15	170.42	164.38
16	550.68	203.93
17	191.52	148.08
18	190.31	155.58
19	148.37	157.85
20	180.33	166.42

Table 6

Distribution and Branch Line Length Approximations of NNIM-LLA for the Rural Case and Default Operation Settings B' for Different L1PMA Numbers of Monotonic Sections when a_{CUD} Values of CUD Measurements range from 1dB to 20dB

L1PMA Number of Monotonic Sections	Maximum RMSD Difference between the Best Values (m) (Default Operation Settings B': 127.26m) (Default Operation Settings C': 93.71m)	Mean RMSD (m) (Default Operation Settings B': 99.57m) (Default Operation Settings C': 96.98m)
1	100.24	95.82
2	116.38	97.78
3	252.16	100.47
4	178.65	106.13
5	237.15	89.21
6	94.16	101.73
7	128.24	101.48
8	217.56	105.02
9	189.85	99.59
10	224.98	115.85

11	98.55	102.35
12	120.74	90.33
13	145.04	87.71
14	181.69	103.53
15	145.69	98.98
16	181.15	104.00
17	120.28	103.75
18	116.41	104.33
19	114.11	93.58
20	144.43	95.82

Similarly to Tables 1 and 3, NNIM-LLA gives approximations of the distribution and branch line lengths of the suburban case in Table 7 when the default operation settings B' are adopted, L1PMA of PMDAM with 10 monotonic sections is activated prior to the NNIM-LLA and the same a_{CUD} values of CUD measurements of Tables 1 and 3 are assumed. Also, the best RMSD value between the approximated original and symmetrical OV LV topologies and the respective OV LV BPL suburban topology are presented per a_{CUD} value. Table 8 is similar to Table 7 but for the rural case when L1PMA of PMDAM with 6 monotonic sections is activated.

From Tables 7 and 8, it is verified that the L1PMA application may allow better mitigation performance of the measurement differences in comparison with the performance of only applying default operation settings B' but a careful selection of monotonic sections is required, which is anyway a difficult task when NN algorithms follow the PMDAM operation. Conversely, the L1PMA application does not achieve better mitigation performance of the measurement differences in comparison with the performance of only applying default operation settings C'. But, it should be noted that the total duration time for preparing both Tables 7 and 8 is equal to 1416s when L1PMA and default operation settings B' are adopted that is anyway significantly lower than 10,048s of preparing the respective Tables 3 and 4 when the default operation settings C' are adopted.

Table 7

Distribution and Branch Line Length Approximations of NNIM-LLA for the Suburban Case, Default Operation Settings B' and L1PMA of 10 Monotonic Sections for Different a_{CUD} Values of CUD Measurements (the symmetrical approximations are reported in blue font color and the suburban case is included in the TIM OV LV BPL topology database)

Indicative OV LV BPL Topologies of Table 1 of [1]		Suburban Case	RMSD	Notes
Distribution Line Length L =$[L_1 \quad L_2 \quad L_3 \quad 0]$ **Branch Line Length L$_b$** =$[L_{b1} \quad L_{b2} \quad 0]$		[500m 400m 100m 0m] [50m 10m 0m]	-	-
NNIM-LLA **Approximated Distribution Line Length** $L_{NNIM-LLA} =$ $[L_{1,NNIM-LLA} \quad L_{2,NNIM-LLA} \quad L_{3,NNIM-LLA} \quad 0]$ **Approximated Branch Line Length** $L_{b,NNIM-LLA} =$ $[L_{b1,NNIM-LLA} \quad L_{b2,NNIM-LLA} \quad 0]$	a_{CUD} **of CUD Measurements (dB)**			Default Operation Settings B' + 1 hidden layer +L1PMA (10 monotonic sections)
	0	[36]1.25m 92.91m 195.84m 0m] [146.14m 139.60m 0m]	157.73m	
	1	[721.59m 70.38m 208.02m 0m] [168.39m 171.17m 0m]	172.96m	
	2	[36]6.27m 78.62m 205.11m 0m] [151.49m 148.70m 0m]	165.03m	
	3	[750.48m 34.69m 214.82m 0m] [151.82m 149.2m 0m]	184.82m	
	4	[700.04m 99.81m 200.14m 0m] [143.47m 141.51m 0m]	154.08m	
	5	[701.93m 100.58m 197.49m 0m] [139.43m 143.54m 0m]	153.89m	
	6	[36]7.19m 71.79m 211.02m 0m] [145.24m 154.62m 0m]	167.84m	
	7	[211.77m 728.54m 59.69m 0m] [155.44m 152.73m 0m]	178.94m	
	8	[36]4.05m 37.94m 248.01m 0m] [34.47m 54.02m 0m]	169.45m	
	9	[731.75m 59.54m 208.71m 0m] [156.03m 157.09m 0m]	174.98m	
	10	[223.17m 724.06m 52.79m 0m] [155.63m 139.29m 0m]	173.93m	
	11	[27]3.94m 70.41m 245.12m 0m] [117.71m 127.27m 0m]	161.18m	
	12	[709.64m 85.87m 204.49m 0m] [148.06m 147.70m 0m]	161.30m	
	13	[225.25m 723.82m 50.92m 0m] [173.68m 145.01m 0m]	175.78m	
	14	[27]9.01m 97.95m 213.04m 0m] [189.25m 197.95m 0m]	166.67m	
	15	[265.06m 658.55m 76.39m 0m] [143.67m 126.54m 0m]	143.90m	
	16	[36]7.72m 56.28m 225.99m 0m] [65.79m 67.21m 0m]	162.54m	
	17	[215.08m 738.84m 46.08m 0m] [153.77m 122.19m 0m]	178.19m	
	18	[448.78m 434.41m 116.81m 0m] [192.89m 185.16m 0m]	88.79m	
	19	[477.56m 376.06m 146.39m 0m] [132.08m 118.15m 0m]	55.63m	

| | 20 | [200.05m 754.74m 45.21m 0m] [170.11m 128.41m 0m] | 187.94m | |

Table 8
Distribution and Branch Line Length Approximations of NNIM-LLA for the Rural Case, Default Operation Settings B' and L1PMA of 6 Monotonic Sections for Different a_{CUD} Values of CUD Measurements (the symmetrical approximations are reported in blue font color and the rural case is included in the TIM OV LV BPL topology database)

Indicative OV LV BPL Topologies of Table 1 of [1]		Rural Case	RMSD	Notes
Distribution Line Length L $=[L_1 \quad L_2 \quad 0 \quad 0]$ **Branch Line Length L$_b$** $=[L_{b1} \quad 0 \quad 0]$		[600m 400m 0m 0m] [300m 0m 0m]	-	-
NNIM-LLA **Approximated Distribution Line Length** $L_{NNIM-LLA} =$ $[L_{1,NNIM-LLA} \quad L_{2,NNIM-LLA} \quad 0 \quad 0]$ **Approximated Branch Line Length** $L_{b,NNIM-LLA} = [L_{b1,NNIM-LLA} \quad 0 \quad 0]$	a_{CUD} **of CUD Measurements (dB)**			Default Operation Settings B' + 1 hidden layer +L1PMA (6 monotonic sections)
	0	[567.23m 340.47m 0m] [43.93m 0m 0m]	100.14m	
	1	[901.25m 174.66m 0m 0m] [219.91m 0m 0m]	145.38m	
	2	[799.60m 200.49m 0m 0m] [2.95m 0m 0m]	154.87m	
	3	[658.73m 339.81m 0m 0m] [128.19m 0m 0m]	72.30m	
	4	[777.12m 246.59m 0m 0m] [167.58m 0m 0m]	101.73m	
	5	[730.17m 287.42m 0m 0m] [186.08m 0m 0m]	78.01m	
	6	[742.86m 257.14m 0m 0m] [142.86m 0m 0m]	96.74m	
	7	[814.28m 185.72m 0m 0m] [157.14m 0m 0m]	126.63m	
	8	[640.86m 363.36m 0m 0m] [127.33m 0m 0m]	68.48m	
	9	[661.92m 420.99m 0m 0m] [113.90m 0m 0m]	74.55m	
	10	[889.51m 149.91m 0m 0m] [190.40m 0m 0m]	150.41m	
	11	[694.01m 293.40m 0m 0m] [225.18m 0m 0m]	60.71m	
	12	[709.27m 260.91m 0m 0m] [187.81m 0m 0m]	79.17m	
	13	[815.67m 184.49m 0m 0m] [81.02m 0m 0m]	141.88m	
	14	[743.26m 249.32m 0m 0m] [59.21m 0m 0m]	120.24m	
	15	[707.03m 354.37m 0m 0m] [130.14m 0m 0m]	77.82m	
	16	[704.34m 303.33m 0m 0m] [122.22m 0m 0m]	86.05m	
	17	[779.61m 217.71m 0m 0m] [183.32m 0m 0m]	106.30m	

	18	[743.38m 192.28m 0m 0m] [219.24m 0m 0m]	100.17m
	19	[772.08m 216.12m 0m 0m] [138.79m 0m 0m]	113.02m
	20	[750.02m 250.11m 0m 0m] [298.27m 0m 0m]	80.16m

As L2WPMA of PMDAM is concerned, similarly to Table 5 of L1PMA, in Tables 9, the maximum RMSD difference between the best values and mean RMSD for the suburban case is reported per monotonic section, which ranges from 1 to 20, when L2WPMA and default operation settings B' are applied and a_{CUD} values of measurement differences range from 1dB to 20dB. Similarly to Table 6 of L1PMA, in Table 10, similar approximation performance metrics are given but for the rural case when L2WPMA and default operation settings B' are applied. Similarly to Tables 6 and 7, the maximum RMSD difference between the best values and the mean RMSD that are lower than the respective values of the default operation settings B' per case are shown in green color while the cases with the lowest maximum RMSD difference between the best values are highlighted in yellow color in Tables 9 and 10.

Table 9
Distribution and Branch Line Length Approximations of NNIM-LLA for the Suburban Case and Default Operation Settings B' for Different L2WPMA Numbers of Monotonic Sections when a_{CUD} Values of CUD Measurements range from 1dB to 20dB

L1PMA Number of Monotonic Sections	Maximum RMSD Difference between the Best Values (m) (Default Operation Settings B': 137.95m) (Default Operation Settings C': 92.26m)	Mean RMSD (m) (Default Operation Settings B': 163.60m) (Default Operation Settings C': 114.60m)
1	238.68	161.43
2	133.91	166.17
3	166.44	150.33
4	503.18	165.03
5	179.32	161.39
6	153.12	169.48
7	166.76	166.20
8	112.38	150.10
9	112.74	156.24
10	140.70	179.77
11	178.16	159.96
12	53.48	173.48
13	248.88	169.05
14	141.12	169.79
15	181.97	163.25
16	213.50	156.58
17	156.26	185.69
18	102.97	166.37
19	137.95	170.37
20	111.46	161.43

Table 10

Distribution and Branch Line Length Approximations of NNIM-LLA for the Rural Case and Default Operation Settings B' for Different L2WPMA Numbers of Monotonic Sections when a_{CUD} Values of CUD Measurements range from 1dB to 20dB

L1PMA Number of Monotonic Sections	Maximum RMSD Difference between the Best Values (m) (Default Operation Settings B': 127.26m) (Default Operation Settings C': 93.71m)	Mean RMSD (m) (Default Operation Settings B': 99.57m) (Default Operation Settings C': 96.98m)
1	142.50	79.87
2	189.54	115.42
3	135.63	110.10
4	317.46	109.18
5	94.38	108.50
6	187.90	115.80
7	187.20	113.90
8	164.55	89.29
9	147.96	100.75
10	235.47	105.82
11	171.38	109.40
12	117.72	109.60
13	162.39	125.97
14	872.65	147.28
15	233.67	125.19
16	219.60	92.21
17	127.40	106.80
18	128.80	88.18
19	127.26	99.68
20	98.61	79.87

In Table 9 where the suburban case is investigated, L2WPMA helps towards the improvement of either the maximum RMSD difference between the best values (i.e. 7 out of 20 cases examined) or the mean RMSD (i.e. 9 out of 20 cases examined) when the careful selection of monotonic sections is made. Actually, in 3 examined cases of Table 9, the application of L2WPMA achieves to improve both the maximum RMSD difference between the best values and the mean RMSD. Similar performance results are observed in the rural case of Table 10. As the numbers of monotonic sections with the lowest maximum RMSD difference between the best values, 12 and 5 monotonic sections are concerned for the suburban and rural cases, respectively, while 20 and 6 monotonic sections have been respectively applied in [25], [27]. Already been mentioned and identified in [25], [27], L1PMA and L2WPMA are both piecewise monotonic data approximations and components of the PMDAM that present similar behavior concerning the selection of the monotonic sections per examined OV LV BPL topology despite their theoretical definition differences; say, higher numbers of monotonic sections are expected when OV LV BPL topologies of more and shorter branches are encountered.

Similarly to Tables 7 and 8, NNIM-LLA gives approximations of the distribution and branch line lengths of the suburban case in Table 11 when the default operation settings B' and L2WPMA with 12 monotonic sections are applied and the same a_{CUD} values of CUD measurements of Tables 1, 3 and 7 are assumed. Also, the best RMSD value between the approximated original and symmetrical OV LV topologies and the

respective OV LV BPL suburban topology are presented per a_{CUD} value. Table 12 is similar to Table 11 but for the rural case when the default operation settings B' and L2WPMA of 5 monotonic sections are applied.

Table 11

Distribution and Branch Line Length Approximations of NNIM-LLA for the Suburban Case, Default Operation Settings B' and L2WPMA of 12 Monotonic Sections for Different a_{CUD} Values of CUD Measurements (the symmetrical approximations are reported in blue font color and the suburban case is included in the TIM OV LV BPL topology database)

Indicative OV LV BPL Topologies of Table 1 of [1]		Suburban Case	RMSD	Notes
Distribution Line Length L $=[L_1 \quad L_2 \quad L_3 \quad 0]$ **Branch Line Length L$_b$** $=[L_{b1} \quad L_{b2} \quad 0]$		[500m 400m 100m 0m] [50m 10m 0m]	-	-
NNIM-LLA **Approximated Distribution Line Length** $\mathbf{L_{NNIM-LLA}} =$ $[L_{1,NNIM-LLA} \quad L_{2,NNIM-LLA} \quad L_{3,NNIM-LLA} \quad 0]$ **Approximated Branch Line Length** $\mathbf{L_{b,NNIM-LLA}} =$ $[L_{b1,NNIM-LLA} \quad L_{b2,NNIM-LLA} \quad 0]$	$\mathbf{a_{CUD}}$ **of CUD Measurements (dB)**			Default Operation Settings B' + 1 hidden layer +L2WPMA (12 monotonic sections)
	0	[188.04m 771.39m 40.57m 0m] [150.63m 128.97m 0m]	193.86m	
	1	[36]5.07m 71.50m 213.43m 0m] [149.51m 142.19m 0m]	166.65m	
	2	[752.06m 36.74m 211.20m 0m] [157.03m 145.04m 0m]	184.22m	
	3	[214.46m 743.14m 42.40m 0m] [172.75m 149.09m 0m]	184.01m	
	4	[700.94m 76.41m 222.65m 0m] [139.91m 151.19m 0m]	163.95m	
	5	[213.49m 740.01m 46.51m 0m] [143.54m 147.21m 0m]	180.53m	
	6	[181.03m 782.64m 36.23m 0m] [154.65m 145.29m 0m]	200.53m	
	7	[213.55m 745.46m 40.99m 0m] [166.60m 122.28m 0m]	181.69m	
	8	[224.62m 722.36m 53.03m 0m] [167.81m 113.32m 0m]	171.76m	
	9	[36]5.06m 74.02m 210.93m 0m] [141.77m 148.54m 0m]	165.80m	
	10	[233.92m 704.59m 61.48m 0m] [169.93m 145.51m 0m]	168.10m	
	11	[36]0.63m 80.57m 208.80m 0m] [146.69m 147.52m 0m]	163.23m	
	12	[223.02m 723.78m 53.21m 0m] [173.72m 141.00m 0m]	175.75m	
	13	[223.15m 736.73m 40.11m 0m] [173.50m 127.07m 0m]	178.32m	
	14	[690.93m 115.86m 193.21m 0m] [139.01m 142.52m 0m]	147.05m	
	15	[36]4.54m 78.36m 207.10m 0m] [145.28m 154.86m 0m]	165.19m	
	16	[212.69m 738.15m 49.17m 0m] [166.44m 118.70m 0m]	179.22m	

	17	[213.24m 728.84m 57.92m 0m] [162.19m 146.09m 0m]	178.58m	
	18	[222.91m 722.87m 54.23m 0m] [161.27m 152.80m 0m]	175.62m	
	19	[734.82m 40.68m 224.50m 0m] [164.86m 148.24m 0m]	182.07m	
	20	[707.92m 97.29m 194.79m 0m] [152.97m 147.45m 0m]	157.36m	

Table 12

Distribution and Branch Line Length Approximations of NNIM-LLA for the Rural Case, Default Operation Settings B' and L2WPMA of 5 Monotonic Sections for Different a_{CUD} Values of CUD Measurements (the symmetrical approximations are reported in blue font color and the rural case is included in the TIM OV LV BPL topology database)

Indicative OV LV BPL Topologies of Table 1 of [1]		**Rural Case**	**RMSD**	**Notes**
Distribution Line Length L $=[L_1 \quad L_2 \quad 0 \quad 0]$ **Branch Line Length** $\mathbf{L_b} =[L_{b1} \quad 0 \quad 0]$		[600m 400m 0m 0m] [300m 0m 0m]	-	-
NNIM-LLA **Approximated Distribution Line Length** $\mathbf{L_{NNIM-LLA}} =$ $[L_{1,NNIM-LLA} \quad L_{2,NNIM-LLA} \quad 0 \quad 0]$ **Approximated Branch Line Length** $\mathbf{L_{b,NNIM-LLA}} = [L_{b1,NNIM-LLA} \quad 0 \quad 0]$	a_{CUD} **of CUD Measurements (dB)**			Default Operation Settings B' + 1 hidden layer +L2WPMA (5 monotonic sections)
	0	[726.69m 283.12m 0m 0m] [178.69m 0m 0m]	79.67m	
	1	[725.80m 274.20m 0m 0m] [151.94m 0m 0m]	87.48m	
	2	[501.71m 497.64m 0m 0m] [181.40m 0m 0m]	68.93m	
	3	[779.14m 238.37m 0m 0m] [66.48m 0m 0m]	126.91m	
	4	[538.48m 210.80m 0m 0m] [135.55m 0m 0m]	97.56m	
	5	[811.12m 177.45m 0m 0m] [27].65m 0m 0m]	145.22m	
	6	[699.43m 270.02m 0m 0m] [189.01m 0m 0m]	74.74m	
	7	[801.41m 199.45m 0m 0m] [187.32m 0m 0m]	155.56m	
	8	[823.41m 763.60m 0m 0m] [254.69m 0m 0m]	162.21m	
	9	[794.92m 272.25m 0m 0m] [171.80m 0m 0m]	100.53m	
	10	[762.50m 237.50m 0m 0m] [150m 0m 0m]	103.73m	
	11	[732.72m 269.18m 0m 0m] [32.17m 0m 0m]	123.32m	
	12	[780.04m 220.83m 0m 0m] [143.68m 0m 0m]	112.73m	
	13	[575.14m 559.29m 0m 0m] [76.26m 0m 0m]	104.23m	
	14	[836.89m 124.36m 0m 0m] [301.10m 0m 0m]	137.37m	

	15	[773.05m 223.89m 0m 0m] [7.56m 0m 0m]	144.66m	
	16	[425.06m 375.05m 0m 0m] [268.79m 0m 0m]	67.83m	
	17	[704.19m 295.81m 0m 0m] [86.19m 0m 0m]	98.15m	
	18	[656.53m 309.71m 0m 0m] [102.55m 0m 0m]	84.80m	
	19	[728.78m 271.18m 0m 0m] [4.14m 0m 0m]	131.32m	
	20	[36]2.50m 287.50m 0m 0m] [150m 0m 0m]	82.65m	

From Tables 11 and 12, it can be generalized that the application of piecewise monotonic data approximations may allow better mitigation performance of the measurement differences in comparison with the performance of only applying default operation settings B' but this performance cannot surpass the one of only applying more elaborate default operation settings, such as default operation settings C'. Known the number of monotonic sections, which remains a challenge anyway, the main advantage of deploying piecewise monotonic data approximations against measurement differences is their light total duration time aggravation; the total duration time for preparing both Tables 11 and 12 is equal to 1,423s for L2WPMA and default operation settings B' that is almost equal to the duration time of applying L1PMA and default operation settings B' but it is again significantly lower than 10,048s of preparing the respective Tables 3 and 4 when the default operation settings C' are adopted.

3.3 Piecewise Monotonic Data Approximations against Measurement Differences in a NN Environment - Discussion

To graphically validate the mitigation performance of the application of L1PMA against the CUD measurement differences when various a_{CUD} values are applied, which has been reported in Tables 5-12, the best RMSD values of the NNIM-LLA approximations for the suburban case are plotted in Fig. 1(a) with respect to the a_{CUD} of the applied CUD measurements when the default operation settings B', the default operation settings C' and the combined operation of L1PMA of 10 monotonic sections with the default operation settings B' are applied. In Fig. 1(a), Tables 1, 3 and 7 are exploited for curving the plots of the default operation settings B', the default operation settings C' and the combined application of L1PMA with the default operation settings B', respectively, when one hidden layer is applied. In Fig. 1(b), the same plot with Fig. 1(a) is given but for the rural case by exploiting Tables 2, 4 and 8 for the application of the default operation settings B', the default operation settings C' and the combined operation of L1PMA of 6 monotonic sections with the default operation settings B', respectively. As the application of L2WPMA against the CUD measurement differences is concerned, the best RMSD values of the NNIM-LLA approximations for the suburban case are plotted in Fig. 2(a) with respect to the a_{CUD} of the applied CUD measurements when the default operation settings B', the default operation settings C' and the combined operation of L2WPMA of 12 monotonic sections with the default operation settings B' are applied. In Fig. 2(a), Tables 1, 3 and 11 are exploited for curving the plots of the

default operation settings B', the default operation settings C' and the combined application of L2WPMA with the default operation settings B', respectively, when one hidden layer is applied. In Fig. 2(b), the same plot with Fig. 2(a) is given but for the rural case by exploiting Tables 2, 4 and 12 for the application of the default operation settings B', the default operation settings C' and the combined operation of L2WPMA of 5 monotonic sections with the default operation settings B', respectively.

In Figs. 1 and 2, the mitigation performance of the default operation settings B', the default operation settings C' and the combined operation of L1PMA with the default operation settings B' is graphically synopsized. Concluding this companion paper and with reference to Figs. 1 and 2, the following remarks are pointed out:

- The maximum RMSD difference between the best values has been applied as the criterion or the main mitigation performance metric against the CUD measurement differences of various a_{CUD} values for assessing the default operation settings B', the default operation settings C' and the combined operation of L1PMA / L2WPMA with the default operation settings B'. This performance metric has been chosen so as to focus on the stability of the NNIM-LLA approximations thus bypassing the high number of executions [1]. Figs. 1 and 2 validate that the combined operation of L1PMA / L2WPMA with the default operation settings B' achieves more stable NNIM-LLA approximations in comparison with the ones of simply applying the default operation settings B' with small total duration time increase. However, the selection of the appropriate number of monotonic sections in both piecewise monotonic data approximation methods remains a challenging issue for the different BPL topologies and BPL topology classes. Conversely, Figs. 1 and 2 also verify that the combined operation of L1PMA / L2WPMA with the default operation settings B' achieves less stable NNIM-LLA approximations in comparison with the ones of simply applying the default operation settings C'. Apart from the better maximum RMSD differences between the best values achieved, the default operation settings C' allow better mean RMSDs for the NNIM-LLA approximations but significantly higher total duration times when different segments of the TIM OV LV BPL topology database are required to be prepared in each case.
- Already been identified, other mitigation performance metrics against the CUD measurement differences of various a_{CUD} values that should be taken into account during the assessment of various methodologies are the mean RMSD and the total duration time. In fact, the main mitigation performance metric against the CUD measurement differences of various a_{CUD} values could be the mean RMSD when the accuracy of NNIM-LLA approximations is of interest rather than the NNIM-LLA approximation stability of this companion paper. Anyway, a fair compromise of all the aforementioned mitigation performance metrics is promoted during the assessment in the future works.
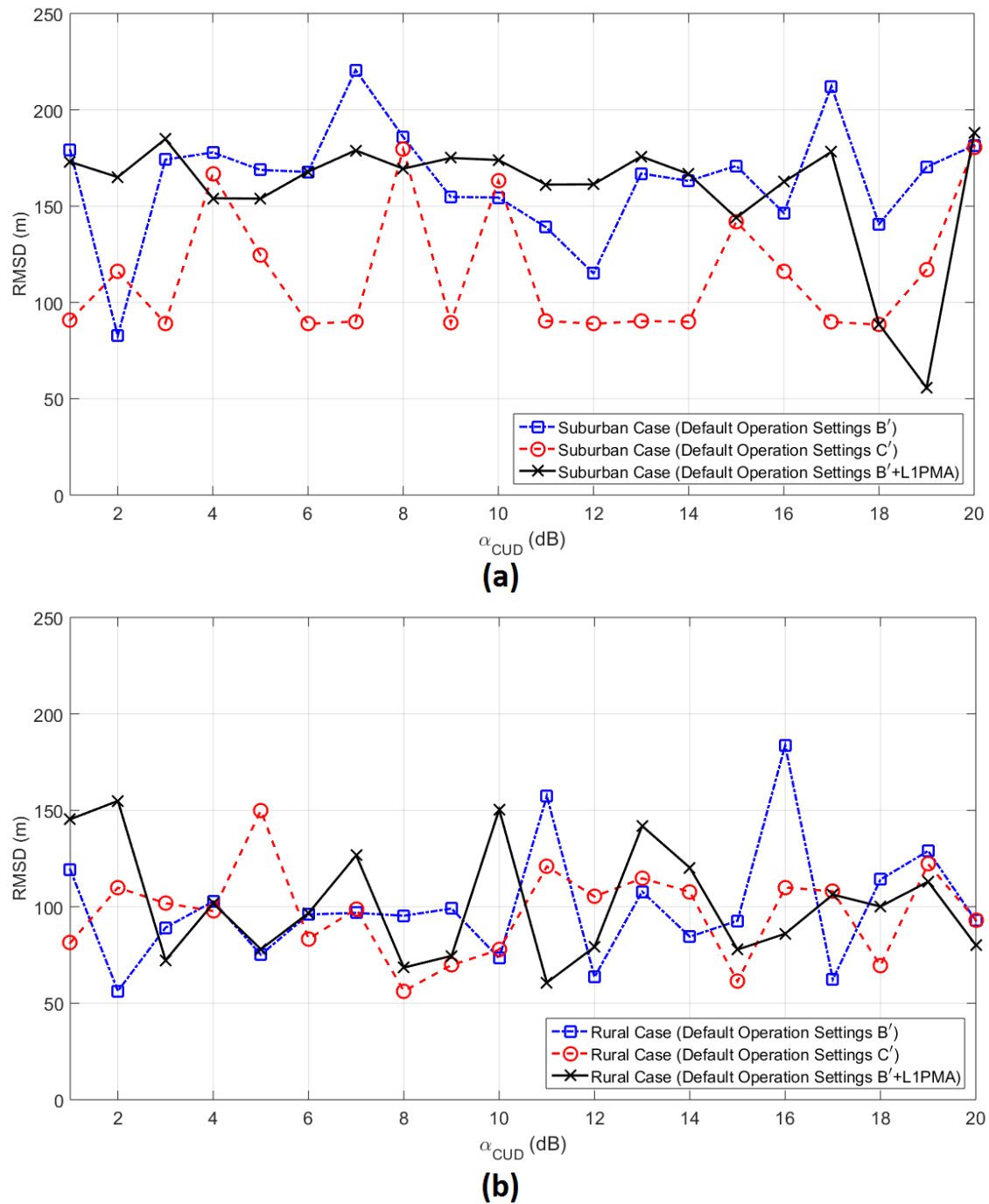
Figure 1. Best RMSD values of NNIM-LLA approximations with respect to a_{CUD} of the applied CUD measurements when the default operation settings B', the default operation settings C' and the combined operation of the default operation settings B' with L1PMA are applied and one hidden layer is assumed. (a) Suburban case -10 monotonic sections for L1PMA-. (b) Rural case - 6 monotonic sections for L1PMA-.
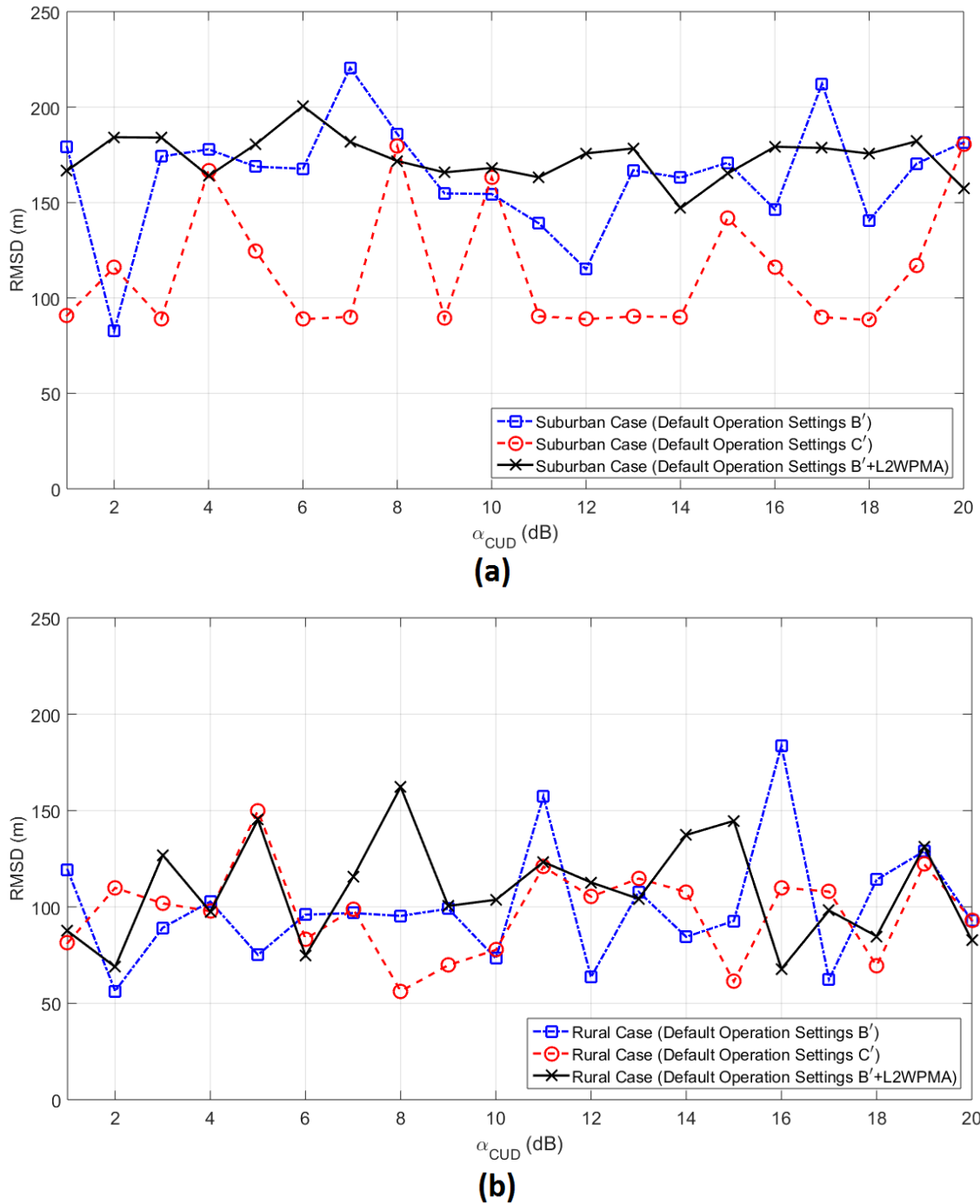
Figure 2. Best RMSD values of NNIM-LLA approximations with respect to a_{CUD} of the applied CUD measurements when the default operation settings B', the default operation settings C' and the combined operation of the default operation settings B' with L2WPMA are applied and one hidden layer is assumed. (a) Suburban case -12 monotonic sections for L2WPMA-. (b) Rural case -5 monotonic sections for L2WPMA-.

- The main constraint of successfully applying piecewise monotonic data approximations, such as L1PMA or L2WPMA of this companion paper, against measurement differences during the operation of NN methodologies is the right selection of monotonic sections. Already been identified in [25], [26], [28], [36], [37], [40], [43], the higher complexity of the examined BPL topologies concerning the number and the length of the branches requires higher number of monotonic sections by the piecewise monotonic data approximations due to the occurred number and depth of notches across the coupling scheme transfer function theoretical numerical results from DHM that are further contaminated with the measurement differences. Although the aforementioned correlation between the complexity of BPL topology classes and the number of monotonic sections still occurs during the combined operation of DHM, PMDAM and NNIM-LLA of this companion, further study and investigation are required towards the use of the adaptive number of monotonic sections, which has been proposed in [25], [27].

- Piecewise monotonic data approximation methods, such as L1PMA and L2WPMA, have theoretically been presented and experimentally verified in [28]-[31], [44]-[46]. Until now, when piecewise monotonic data approximation methods have been applied as the output module they have successfully mitigated the measurement differences in transmission and distribution BPL networks. In this companion paper, piecewise monotonic data approximation methods, which are contained in the PMDAM module, are located prior to the NNIM-LLA module and feed the latter module with the approximated coupling scheme channel transfer function results. However, the applied representative sets of the TIM OV LV BPL topology database, the assumed default operation settings and the operation specifications of the MATLAB NN program of [38], [39] mainly affect the NNIM-LLA approximation performance thus limiting the PMDAM performance improvement.

4. Conclusions

In this companion paper, the mitigation role of the piecewise monotonic data approximation methods against CUD measurement differences of various α_{CUD} values has been assessed when NNIM-LLA approximations are expected for OV LV BPL topologies. In fact, PMDAM module, which contains L1PMA and L2WPMA that are the piecewise monotonic data approximations of interest in this companion paper, acts as the intermediate module after the DHM module and before the NNIM-LLA module. In accordance with the existing literature of piecewise monotonic data approximation methods, the crucial issue of the right selection of the number of monotonic sections of L1PMA and L2WPMA has been recognized while the correlation of the number of monotonic sections with the complexity of the examined OV LV BPL topology classes has also been revealed in this companion paper. It has been shown that the right selection of the applied number of monotonic sections in L1PMA and L2WPMA may improve either the stability of NNIM-LLA approximations through the improvement of the maximum RMSD difference between the best values or the overall performance of NNIM-LLA approximations through the improvement of the mean RMSD. At the same time, the total duration time of NNIM-LLA operation is not significantly affected by the

operation of PMDAM. However, it has been verified that the default operation settings, which affect the preparation of the TIM OV LV BPL topology database and the NNIM-LLA operation, are the dominant factor of the NNIM-LLA approximation performance; say, the best tuning of L1PMA and L2WPMA can improve the NNIM-LLA approximation performance for given default operation settings but it cannot improve the NNIM-LLA approximation performance in comparison with the one of applying more elaborated default operation settings and this is due to: (i) the PMDAM position prior to the NNIM-LLA module; and (ii) the NN definition and operation inside the NNIM-LLA module.

CONFLICTS OF INTEREST

The authors declare that there is no conflict of interests regarding the publication of this paper.

References

[1]   Lazaropoulos, A. G., & Leligou, H. C. (2024). Big Data and Neural Networks in Smart Grid - Part 2: The Impact of Piecewise Monotonic Data Approximation Methods on the Performance of Neural Network Identification Methodology for the Distribution Line and Branch Line Length Approximation of Overhead Low-Voltage Broadband over Powerlines Networks. _Trends in Renewable Energy, 10_, 30-66. doi: https://doi.org/10.17737/tre.2024.10.1.00164

[2]   Qays, M. O., Ahmad, I., Abu-Siada, A., Hossain, M. L., & Yasmin, F. (2023). Key communication technologies, applications, protocols and future guides for IoT-assisted smart grid systems: A review. _Energy Reports, 9_, 2440-2452.

[3]   Lazaropoulos, A. G. (2021). Information Technology, Artificial Intelligence and Machine Learning in Smart Grid – Performance Comparison between Topology Identification Methodology and Neural Network Identification Methodology for the Branch Number Approximation of Overhead Low-Voltage Broadband over Power Lines Network Topologies. _Trends in Renewable Energy, 7_, 87-113. doi: https://doi.org/10.17737/tre.2021.7.1.00133

[4]   Yu, F. R., Zhang, P., Xiao, W., & Choudhury, P. (2011). Communication systems for grid integration of renewable energy resources. _IEEE Network, 25_(5), 22-29.

[5]   Hallak, G., Berners, M., & Mengi, A. (2021). Planning tool for fast roll-out of G.hn broadband PLC in smart grid networks: evaluation and field results. In _2021 IEEE International Symposium on Power Line Communications and Its Applications (ISPLC)_, pp. 108-113.

[6]   Aalamifar, F., & Lampe, L. (2017). Optimized WiMAX profile configuration for smart grid communications. _IEEE Transactions on Smart Grid, 8_(6), 2723-2732.

[7]   Lazaropoulos, A. G. (2014). Wireless sensor network design for transmission line monitoring, metering and controlling introducing broadband over powerlines-enhanced network model (BPLeNM). _ISRN Power Engineering, 2014_, 894628.

[8]   Rehmani, M. H., Reisslein, M., Rachedi, A., Erol-Kantarci, M., & Radenkovic, M. (2018). Integrating renewable energy resources into the smart grid: Recent

developments in information and communication technologies. *IEEE Transactions on Industrial Informatics, 14*(7), 2814-2825.

[9] Heile, B. (2010). Smart grids for green communications [Industry perspectives]. *IEEE Wireless Communications, 17*(3), 4-6.

[10] Muqeet, H. A., Liaqat, R., Jamil, M., & Khan, A. A. (2023). A state-of-the-art review of smart energy systems and their management in a smart grid environment. *Energies, 16(1)*, 472.

[11] Lazaropoulos, A. G., & Leligou, H. C. (2022). Fiber optics and broadband over power lines in smart grid: a communications system architecture for overhead high-voltage, medium-voltage and low-voltage power grids. *Progress in Electromagnetics Research B, 95*, 185-205.

[12] Lazaropoulos, A. G., & Cottis, P. G. (2009). Transmission Characteristics of Overhead Medium-Voltage Power-Line Communication Channels. *IEEE Transactions on Power Delivery, 24*(3)*, 1164-1173. doi: https://doi.org/10.1109/tpwrd.2008.2008467

[13] Lazaropoulos, A. G., & Cottis, P. G. (2010). Capacity of overhead medium voltage power line communication channels. *IEEE Transactions on Power Delivery, 25*(2), 723-733. doi: https://doi.org/10.1109/TPWRD.2009.2038119

[14] Lazaropoulos, A. G. (2012). Towards modal integration of overhead and underground low-voltage and medium-voltage power line communication channels in the smart grid landscape: Model expansion, broadband signal transmission characteristics, and statistical performance metrics (Invited paper). *ISRN Signal Processing, 2012*, 1-17. doi: https://doi.org/10.1155/2012/121628

[15] Lazaropoulos, A. G. (2016). New coupling schemes for distribution broadband over power lines (BPL) networks. *Progress in Electromagnetics Research B, 71*, 39-54.

[16] Amirshahi, P., & Kavehrad, M. (2006). High-frequency characteristics of overhead multiconductor power lines for broadband communications. *IEEE Journal on Selected Areas in Communications, 24*(7), 1292-1303. doi: https://doi.org/10.1109/JSAC.2006.061003

[17] Amirshahi, P. (2006). *Broadband access and home networking through powerline networks*. Ph.D. dissertation, Pennsylvania State University, University Park, PA.

[18] Sartenaer, T. (2004). *Multiuser communications over frequency selective wired channels and applications to the powerline access network*. Doctoral dissertation, Université catholique de Louvain, Louvain-la-Neuve, Belgium.

[19] Sartenaer, T., & Delogne, P. (2006). Deterministic modeling of the (shielded) outdoor powerline channel based on the multiconductor transmission line equations. *IEEE Journal on Selected Areas in Communications, 24*(7), 1277-1291. doi: https://doi.org/10.1109/JSAC.2006.070804

[20] Sartenaer, T., & Delogne, P. (2001). Powerline cables modeling for broadband communications. In *Proceedings of the IEEE International Conference on Power Line Communications and Its Applications*, Malmo, Sweden, April 2001, pp. 331-337.

[21] Lazaropoulos, A. G. (2017). Improvement of Power Systems Stability by Applying Topology Identification Methodology (TIM) and Fault and Instability Identification Methodology (FIIM) - Study of the Overhead Medium-Voltage Broadband over Power Lines (OV MV BPL) Networks Case. *Trends in Renewable Energy, 3*, 102-128. doi: https://doi.org/10.17737/tre.2017.3.2.0034

[22] Lazaropoulos, A. G. (2016). Measurement Differences, Faults and Instabilities in Intelligent Energy Systems - Part 1: Identification of Overhead High-Voltage Broadband over Power Lines Network Topologies by Applying Topology Identification Methodology (TIM). _Trends in Renewable Energy, 2_, 85-112. doi: https://doi.org/10.17737/tre.2016.2.3.0026

[23] Lazaropoulos, A. G., & Leligou, H. C. (2023). Artificial intelligence, machine learning and neural networks for tomography in smart grid - performance comparison between topology identification methodology and neural network identification methodology for the distribution line and branch line length approximation of overhead low-voltage broadband over power lines network topologies. _Trends in Renewable Energy, 9,_ 34-77. doi: https://doi.org/10.17737/tre.2023.9.1.00149

[24] Lazaropoulos, A. G. (2016). Measurement Differences, Faults and Instabilities in Intelligent Energy Systems - Part 2: Fault and Instability Prediction in Overhead High-Voltage Broadband over Power Lines Networks by Applying Fault and Instability Identification Methodology (FIIM). _Trends in Renewable Energy, 2_, 113-142. doi: https://doi.org/10.17737/tre.2016.2.3.0027

[25] Lazaropoulos, A. G. (2017). Main Line Fault Localization Methodology in Smart Grid - Part 2: Extended TM2 Method, Measurement Differences and L1 Piecewise Monotonic Data Approximation for the Overhead Medium-Voltage Broadband over Power Lines Networks Case. _Trends in Renewable Energy, 3_, 26-61. doi: https://doi.org/10.17737/tre.2017.3.3.0037

[26] Lazaropoulos, A. G. (2017). Main Line Fault Localization Methodology in Smart Grid - Part 1: Extended TM2 Method for the Overhead Medium-Voltage Broadband over Power Lines Networks Case. _Trends in Renewable Energy, 3_, 2-25. doi: https://doi.org/10.17737/tre.2017.3.3.0036

[27] Lazaropoulos, A. G. (2020). Business Analytics and IT in Smart Grid - Part 3: New Application Aspect and the Quantitative Mitigation Analysis of Piecewise Monotonic Data Approximations on the iSHM Class Map Footprints of Overhead Low-Voltage Broadband over Power Lines Topologies Contaminated by Measurement Differences. _Trends in Renewable Energy, 6_, 214-233. doi:10.17737/tre.2020.6.2.00119

[28] Lazaropoulos, A. G. (2016). Best L1 piecewise monotonic data approximation in overhead and underground medium-voltage and low-voltage broadband over power lines networks: Theoretical and practical transfer function determination. _Hindawi Journal of Computational Engineering, 2016_, 6762390, 24 pp. doi: https://doi.org/10.1155/2016/6762390

[29] Demetriou, I. C., & Powell, M. J. D. (1991). Least squares smoothing of univariate data to achieve piecewise monotonicity. _IMA Journal of Numerical Analysis, 11_, 411-432.

[30] Demetriou, I. C., & Koutoulidis, V. (2013). On signal restoration by piecewise monotonic approximation. In _Lecture Notes in Engineering and Computer Science: Proceedings of The World Congress on Engineering 2013_, London, U.K., July 2013, pp. 268-273.

[31] Demetriou, I. C. (1994). Best L1 piecewise monotonic data modelling. _International Transactions on Operational Research, 1_(1), 85-94.

[32]   Demetriou, I. C. (2013). An application of best _L_1 piecewise monotonic data approximation to signal restoration. _IAENG International Journal of Applied Mathematics, 53_(4), 226-232.

[33]   Demetriou, I. C. (2003). L1PMA: A Fortran 77 package for best L1 piecewise monotonic data smoothing. _Computer Physics Communications, 151_(1), 315-338.

[34]   Demetriou, I. C. (1985). _Data smoothing by piecewise monotonic divided differences_, Ph.D. dissertation. University of Cambridge, Cambridge.

[35]   Demetriou, I. C. (2007). Algorithm 863: L2WPMA, a Fortran 77 package for weighted least-squares piecewise monotonic data approximation. _ACM Transactions on Mathematical Software, 33_(1), 6.

[36]   Lazaropoulos, A. G. (2017). Power Systems Stability through Piecewise Monotonic Data Approximations - Part 1: Comparative Benchmarking of L1PMA, L2WPMA and L2CXCV in Overhead Medium-Voltage Broadband over Power Lines Networks. _Trends in Renewable Energy, 3_(1), 2-32. doi: https://doi.org/10.17737/tre.2017.3.1.0029

[37]   Lazaropoulos, A. G. (2018). Smart Energy and Spectral Efficiency (SE) of Distribution Broadband over Power Lines (BPL) Networks - Part 2: L1PMA, L2WPMA and L2CXCV for SE against Measurement Differences in Overhead Medium-Voltage BPL Networks. _Trends in Renewable Energy, 4_, 185-212. doi: https://doi.org/10.17737/tre.2018.4.2.0077

[38]   Okoh, D. (2016). _Computer neural networks on MATLAB_. CreateSpace Independent Publishing Platform.

[39]   Okoh, D. (2023). _Neural Network Training Code_ (https://www.mathworks.com/matlabcentral/fileexchange/59362-neural-network-training-code), MATLAB Central File Exchange. Accessed on November 17, 2023.

[40]   Lazaropoulos, A. G. (2020). Business analytics and IT in smart grid - Part 2: The qualitative mitigation impact of piecewise monotonic data approximations on the iSHM class map footprints of overhead low-voltage broadband over power lines topologies contaminated by measurement differences. _Trends in Renewable Energy, 6_, 187-213. doi: https://doi.org/10.17737/tre.2020.6.2.00118

[41]   Lazaropoulos, A. G. (2019). Special cases during the detection of the hook style energy theft in overhead low-voltage power grids through HS-DET method - Part 2: Different measurement differences, feint "smart" hooks, and hook interconnection issues. _Trends in Renewable Energy, 5_(1), 90-116. doi: 10.17737/tre.2019.5.1.0083

[42]   Lazaropoulos, A. G. (2012). Deployment concepts for overhead high voltage broadband over power lines connections with two-hop repeater system: Capacity countermeasures against aggravated topologies and high noise environments. _Progress in Electromagnetics Research B, 44_, 283-307.

[43]   Lazaropoulos, A. G. (2020). Business Analytics and IT in Smart Grid - Part 1: The Impact of Measurement Differences on the iSHM Class Map Footprints of Overhead Low-Voltage Broadband over Power Lines Topologies. _Trends in Renewable Energy, 6_, 156-186. doi: https://doi.org/10.17737/tre.2020.6.2.00117

[44]   Davos, D. E., & Demetriou, I. C. (2022). Convex-concave fitting to successively updated data and its application to covid-19 analysis. _Journal of Combinatorial Optimization, 44_(5), 3233-3262.

[45]   Demetriou, I. C. (2022). A binary search algorithm for univariate data approximation and estimation of extrema by piecewise monotonic constraints. *Journal of Global Optimization, 82*(4), 691-726.

[46]   Vassiliou, E. E., & Demetriou, I. C. (2022). Piecewise monotonic data approximation: Spline representation and linear model-basic statistics. *IAENG International Journal of Applied Mathematics, 52*(1), March 2022.